INTERNATIONAL SOCIETY FOR
SOIL MECHANICS AND
GEOTECHNICAL ENGINEERING

This paper was downloaded from the Online Library of the International Society for Soil Mechanics and Geotechnical Engineering (ISSMGE). The library is available here:

https://www.issmge.org/publications/online-library

This is an open-access database that archives thousands of papers published under the Auspices of the ISSMGE.

The paper was published in the proceedings of the 11th International Conference on Physical Modelling in Geotechnics (ICPMG2026) and was edited by Ioannis Anastasopoulos. The conference was held from June 8th to June 12th 2026 in Zurich, Switzerland.

Monitoring of Strain Behaviour of Geotextile Tubes under Wave Load in Hydraulic Wave Flume

Soon Hoe Chew, Zhuofu Jiang*, Jun Ming Soh, Chuanjin Tang
National University of Singapore, Singapore, Singapore

* *e1010620@u.nus.edu*

ABSTRACT: Geosynthetic containers, such as geotextile bags and geotextile tubes, have been widely used in hydraulic and coastal engineering applications. While many studies have focused on the structure stability of these systems under various field scenarios with wave action, limited research has addressed the strain behavior of the geotextile sheet that made up the tubes under such action. This study aims to investigate the mechanical response of geotextile tube, and the strain development of the geotextile sheet under wave loading through a series of physical model tests. The experiments will be conducted in the 36 m long, 2 m width Ferrocement Flume at the National University of Singapore. A custom-made geotextile tubes made by non-woven geotextile was used in this study. To avoid the hydraulic scaling issue, the strong grade of typical geotextile used in the field (T ≈ 200 kN/m) was scaled down according to the wave load. Hence, a much weaker non-woven geotextile was selected to fullfil the scaling law. The strain behavior in both the longitudinal and transvese directions of the tube is monitored during pumping and wave loading stage. The results of this study will provide valuable insights into the material-level performance of geotextile tubes under wave action, offering a practical reference for the design and application of geotextile tubes in coastal and hydraulic engineering.

1 INTRODUCTION

Geotextile tubes are now widely used as breakwaters, revetments and various coastal and offshore structures. Based on field experience, Lawson (2008) proposed nine typical failure modes of geotextile tubes, which include both external and internal mechanisms. Most recent studies so far have focused on external stability of geotextile tubes under wave loading. For example, the flume tests by van Steeg and Vastenburg (2010) and by Kriel (2012) treated geotextile tubes as low-crested breakwaters and examined sliding, overturning and other global instabilities. In contrast, internal failure modes such as geotextile skin rupture and enrosion of infill material have received much less attention.

In practice, a geotextile tube used as a coastal or offshore structure is exposed to long-term cyclic wave loading. A single storm may not directly cause geotextile rupture, but long-term cyclic wave loading subjects the geotextile fabric to repeated tensile loading–unloading cycles, which can accelerate strain accumulation and fatigue degradation of the material. However, the magnitude of strain variation that geotextile tubes experience under continuous wave loading is still unclear and not well reported. To address this gap, the present study monitors the strain behaviour of geotextile tubes under controlled wave loading in the hydraulic wave flume at the National University of Singapore. A two-layer stack of geotextile tubes filled with cemented kaolin slurry was instrumented with electrical resistance strain gauges in both longitudinal and transverse directions. The recorded strain histories during pumping and under a sequence of wave conditions are used to examine how wave loading influences tube strain and to provide initial insight into internal stability

2 MATERIAL AND SAMPLE PREPARATION

2.1 Geotextile

To choose the proper geotextile fabrics, scaling effect must be taken into consideration so that the physical model simulates the similar prototypes' stress-strain behaviour. In this study, a scaling ratio of approximately 5 was adopted. At this scale, a two-layer geotextile-tube model would correspond to a prototype revetment height of about 1.5-2 m. The value of N equals to 5 was therefore assumed hypothetically to represent this realistic design scenario.

We have the following scaling relationships apply:

$$L_m = \frac{1}{N} L_p \qquad (1)$$

$$M_m = \frac{1}{N^3} M_p \quad (2)$$

Where L_m and L_p are the characteristic lengths of the model and prototype, M_m and M_p are the corresponding masses

Based on Newton's second law,

$$F_m = M_m a = \frac{1}{N^3} M_p a = \frac{1}{N^3} F_p \quad (3)$$

Where F_m and F_p are the forces acting on the model and prototype, and a is acceleration, which is kept constant between model and prototype.

The tensile strength (T) of geotextiles is always expressed in force per unit length. As a result, its scaling relation is:

$$T_m = \frac{F_m}{L_m} = \frac{1}{N^2} \frac{F_p}{L_p} = \frac{1}{N^2} T_p \quad (4)$$

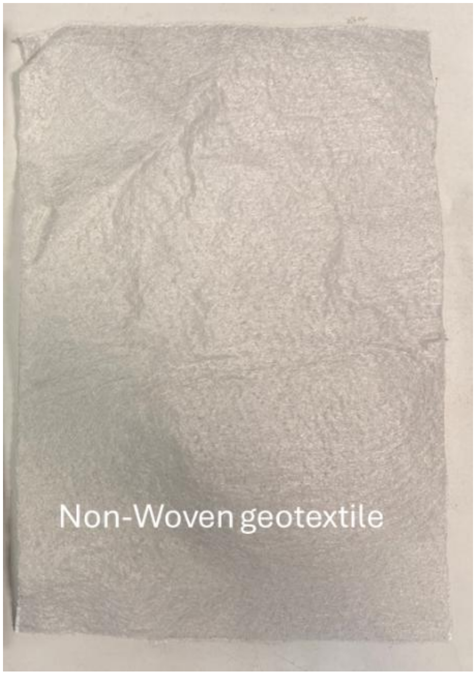

Figure 1. Non-woven geotextile used in the model tests.

Thus, to achieve similitude, the tensile strength of the model fabric should be about $1/N^2$ of the intended prototype fabric. In current practice, most commercial fabrics used for geotextile tubes have strengths on the order of 200-800 kN/m, whereas some high strength wovens exceed 1,000 kN/m. Considering this scaling with N=5, the corresponding tensile strength of geotextile used in modeling should be in the range of 8-32 kN/m. Therefore, a relatively lower-strength commercial woven geotextiles was selected for the model tests to ensure that the model and prototype exhibit comparable mechanical behavior under wave loading. The non-woven geotextile is shown in Figure 1, and its properties are listed in Table 1.

Table 1. Key properties of the non-woven geotextile.

Properties	Unit	Non-woven Fabric
Tensile strength (MD)	kN/m	9.5
Tensile strength (TD)	kN/m	9.5
Puncture Strength	N	1500
Characteristic opening size	mm	O90 = 0.12
Mass per unit area	g/m²	125

2.2 Filling material

Besides the geotextile fabric, the filling material is another important component of a geotextile tube. Sand is the conventional filling material of geotextile tubes and is often taken directly from the construction site or seabed. However, as an island country, Singapore is facing the shortage of sand resources. Therefore, soft soil has been considered as an alternative filling material. Soft-soil–filled tubes, however, have lower shear strength and higher compressibility than sand-filled tubes, which can cause large settlements or even structural instability under loading (Chew et al., 2023). To improve their performance, a small amount of cement can be mixed with the soft soil to form a lightly cemented material (Chew et al., 2025).

In this study, the cement-treated soft soil was chosen as the filling material for Singapore's coastal applications.The soft soil was prepared using kaolin clay powder mixed with water at a mass ratio of 1:2 (kaolin: water). Before the pumping stage, 5% cement by the total mass of kaolin mixture was added into the slurry to treat the soft soil. The 7-day unconfined compressive strength (UCS) of the wet-cured cement-treated kaolin specimen was approximately 28 kPa and the bulk density was about 1.3 g/cm³

2.3 Strain gauge location

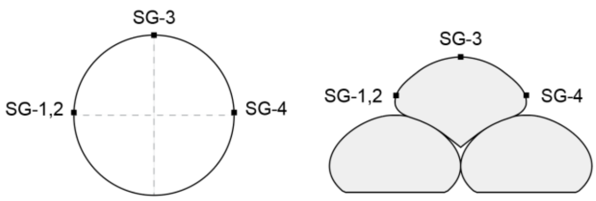

Figure 2. Positioning of strain gauges on geptextile tubes.

To monitor the strain behaviour of the geotextile tube during filling and subsequent wave loading, four electrical resistance strain gauges (SG-1 to SG-4) were installed on the geotextile of the upper tube only as shown in Figure 2. Two principal directions were considered: the longitudinal direction of the (LD) and the circumferential direction (CD) of the tube. By combining these two orientations, the strain gauges are able to capture both the circumferential strain around the tube section and the lateral strain along the tube surface throughout the tests.

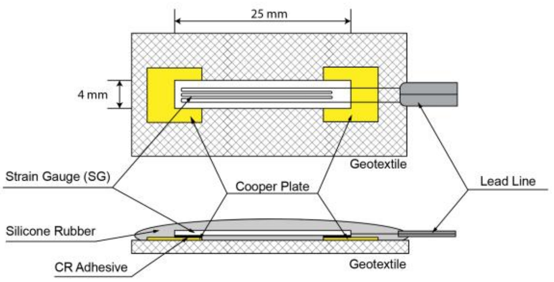

Figure 3. Strain gauge installation detail.

The general installation method of the strain gauges is illustrated in Figure 3, which is modified based on the external gauge attachment method proposed by Chew et al. (2000). First, two copper plates were bonded directly onto the outer surface of the geotextile using an epoxy adhesive. A layer of silicone rubber (KE-348T) was then applied between the cooper plates to provide waterproofing on the back side of the strain gauge. The strain gauge was then bonded across the gap between the two plates, with both ends fixed onto the plates using CR adhesive. Finally, an external coating of silicone rubber was also applied over the gauge and plates to form an overall continuous waterproof layer to protect the strain gauge inside.

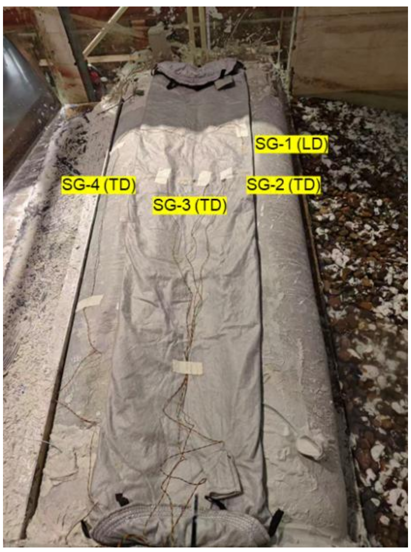

Figure 4. Strain gauge setup on the upper geotextile tube.

As the upper layer tube was directly exposed to the incoming waves and was expected to experience the largest deformation, strain gauges were all applied on this tube. On this tube, SG-1 and SG-2 were positioned on the seaward face at mid-height. SG-1 was aligned with the LD and SG-2 to SG-4 was aligned with the CD at both sides and crown of the tube to measure circumferential strain at three locations. The overall setup is shown in Figure 4.

3 EXPERIMENT SETUP

The physical model tests were conducted in the wave flume at the Hydraulic Laboratory of the National University of Singapore. The flume is 36 m long, 2.0 m wide and 1.3 m high, and is equipped with a piston-type wavemaker capable of generating regular waves over a range of heights and frequencies.

The tested structure consisted of a 2-layers stacking of non-woven geotextile tubes filled with cemented kaolin slurry. Each tube was 2.0 m long with a theoretical circumference of 1.0 m. The stack was placed on a rigid supporting structure 0.5 m high, representing an existing bottom part of revetment. The seaward face of the support was shaped as a rock revetment with a slope of 2H:1V, so that wave transformation and loading on the tubes were similar to those on a typical coastal slope.

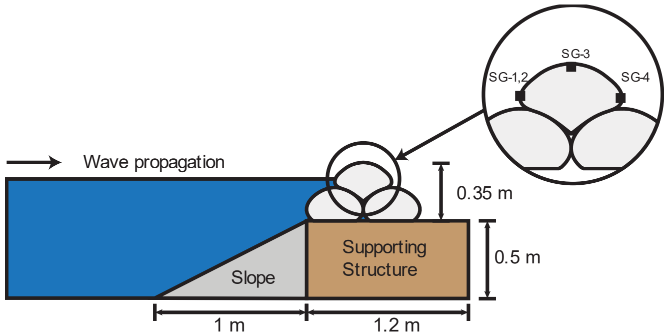

Figure 5. Flume experiment setup.

After filling and curing of the cemented kaolin for 24 hours, the geotextile tube system was then subjected to a series of regular wave actions with progressively increasing wave energy. The wave height and frequency parameters are shown in Table 2. For each wave condition, 1,000 regular waves were generated at a constant water depth of 0.77 m. Throughout the entire test, strain data from the four gauges on the crest tube were recorded continuously using a TSM-530 data logger at a data capturing rate of 1 Hz during both the filling stage and all subsequent wave runs.

Table 2. Wave parameters for all wave conditions applied in the test.

Wave Condition	Wave Height (m)	Frequency (HZ)
C-1	0.1	0.8
C-2	0.12	0.67
C-3	0.14	0.6
C-4	0.16	0.55
C-5	0.18	0.5
C-6	0.20	0.5
C-7	0.22	0.45

4 PRELIMINARY RESULT

Before presenting the results, we note that SG-1 showed some irregular readings, so only the circumferential strain data from SG-2 to SG-4 are discussed in this section.

4.1 Strain behaviour at pumping stage

During the pumping stage, the strain vs. Time variation show three clear "steps" as shown in Figure 6. Each "step" corresponds to one filling sub-stage, because pumping had to be paused whenever the filling material ran out and a new batch of filling material was prepared. At the moment when pumping restarted, the strain at all locations increased sharply, followed by partial relaxation during the pause. In the first two "steps", this relaxation is relatively mild because the tube had not yet been fully filled and the internal pressure could dissipate quickly. In the final "step", that was when the tube approaching its final filling level, the strain at all gauges reached a pronounced peak and then dropped by roughly 15–20%, as the excess pressure induced by pumping gradually dissipated through the voids in the geotextile.

Overall, SG-4 at the landward side recorded the largest circumferential strain, SG-3 at the crown showed intermediate values, and SG-2 on the seaward side remained the lowest. In theory, SG-2 and SG-4 should experience similar strain because they are positioned on opposite sides of the same tube cross-section. The lower readings at SG-2 are likely influenced by local wrinkles on the non-woven geotextile around that gauge, which may reduce the strain transferred to the sensor. Despite this difference in magnitude, the three transverse gauges exhibit similar stepwise trends, indicating a consistent response of the tube to the staged pumping process.

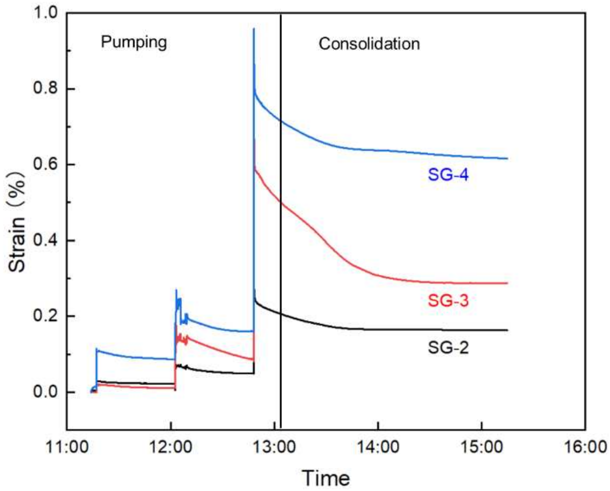

Figure 6. Strain behaviour at pumping stage.

4.2 Strain behaviour at wave loading stage

During the wave loading stage, all three gauges remained largely stable over the seven test wave conditions C-1 to C-7 with only small fluctuations as shown in Figure 7. This suggests that wave loading does not cause large extra stretching in the geotextile fabric. A likely reason is that the cement in the slurry bonds with the non-woven geotextile, so the tube and the infill material act together as one body and the wave load is taken by the whole tube rather than taken only by the geotextile fabric. Additionally, the strain response is also uniform along the whole tube. Although the strain at SG-2 on the seaward side fluctuates slightly more than that at SG-3 and SG-4 because the wave load acts directly on this face, similar fluctuation patterns can still be observed at the crown (SG-3) and on the landward side (SG-4). Overall, by the end of the tests, the strain values on all locations remains almost unchanged compared with the values in early pumping – consolidation stage.

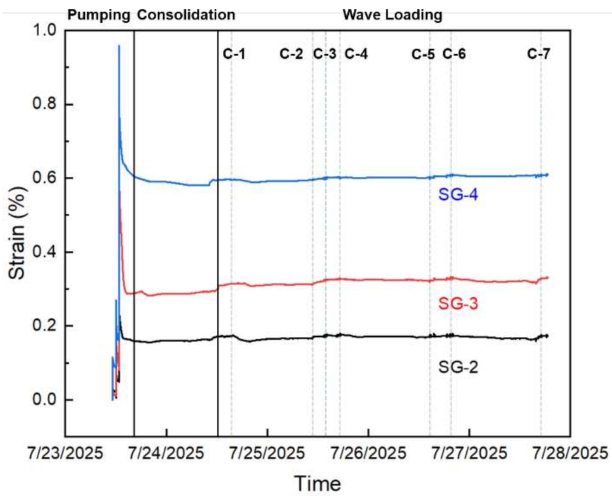

Figure 7. Overall strain behaviour during the test.

The irregular readings from SG-1 are mainly concentrated between the pumping and consolidation stages. A pronounced drop in strain is observed immediately after the completion of pumping, and the measured strain becoming even smaller than the initial value. The underlying reason for this irregular behaviour is not clear, which makes the longitudinal strain response of the geotextile during the pumping and consolidation stages difficult to interpret. Nevertheless, during the wave loading stage, the longitudinal strain exhibits a trend and magnitude that are very similar to those of the circumferential strain.

5 CONCLUSIONS

The results show that wave loading does not cause excessive strain in the geotextile fabric. The strain levels during all wave conditions remain the same level to those recorded after consolidation. This behaviour is likely due to the bonding between the cemented infill and the geotextile fabric, which allows the tube to act as a single unit so that the wave load is resisted by the whole tube.

In contrast, the pumping stage is the most critical period as the highest strain values occur near the final pumping stage when the internal pressure has not yet dissipated. This suggests that the filling process poses more risk of overstretching the geotextile than the wave loading. Although the waves do not significantly variate the strain in the geotextile fabric, their long-term influence on its stability is still uncertain. The results of this study provide a useful reference, but a more complete understanding of wave effects on geotextile tubes will need further study that cover different geotextile types and different filling materials.

ACKNOWLEDGEMENTS

The authors are grateful to the National Research Foundation of Singapore, PUB (Singapore’s National Water Agency) for supporting this work done in the Coastal Protection and Flood Resilience Institute (CFI) Singapore under the Coastal Protection and Flood Management Research Programme (CFRP). The geotextile tubes used in the experiments were supplied by Solmax Geosynthetics Asia Sdn. Bhd. The authors would also like to express their sincere thanks to Mr. Albert Lim Lum Kong and Mr. Ricky Wong Choong Lum for their kind support and assistance in providing the geotextile tube samples. The conclusions put forward in this publication reflect the views of the authors alone and not necessarily CFI Singapore or any of the supporting entities.

REFERENCES

Chew, S. H., Soh, J. M., Lim, Y. M., Deng, J., Tan, Y. C., Yim, A., ... & Chang, D. (2025). Investigation of durability of geotextiles tubes in marine conditions. In *E3S Web of Conferences* (Vol. 644, p. 01006). EDP Sciences.

Chew, S. H., Soh, J. M., Tan, Y. C., Yim, H. M. A., Quek, J. W. A., Lim, D. J., & Kee, S. (2023). Case study of geotextile tubes infilled with recycled excavated soft soil for coastal bund. In *Smart Geotechnics for Smart Societies* (pp. 794-799). CRC Press.

Chew, S. H., Wong, W. K., Ng, C. C., Tan, S. A., & Karunaratne, G. P. (2000). *Strain gauging geotextiles using external gauge attachment method*.

Kriel, H. J. (2012). *Hydraulic stability of multi-layered sand-filled geotextile tube breakwaters under wave attack* (Doctoral dissertation, Stellenbosch: Stellenbosch University).

Lawson, C. R. (2008). Geotextile containment for hydraulic and environmental engineering. *Geosynthetics International*, *15*(6), 384-427.

Van Steeg, P., & Vastenburg, E. W. (2010). *Large scale physical model tests on the stability of geotextile tubes*. Deltares